Med. & biol. Engng. Vol. 7, pp. 169–184. Pergamon Press, 1969. Printed in Great Britain

OXYGEN AND CARBON DIOXIDE TRANSFER IN MEMBRANE OXYGENATORS†

M. H. WEISSMAN‡ and L. F. MOCKROS
Technological Institute, Northwestern University, Evanston, Illinois, U.S.A.

Abstract—Gas transfer in membrane oxygenators can be limited by the liquid dispersion or the membrane diffusion. If limited by liquid dispersion, the increase in average oxygen saturation of blood flowing in straight gas-permeable tubes is dependent upon the flow rate, the tube length, and the diffusion coefficient and independent of the tube diameter. The mathematical solution is surprisingly insensitive to shifts of the oxyhemoglobin dissociation curve. The assumptions utilized in the model and the analytic solution were verified by a series of experiments using cattle blood. Tube staging, turbulence, and tube coiling bring about mixing and significantly improve the oxygenation rate. For coiled tubes, the oxygenation efficiency depends on the Reynolds number, the Schmidt number, and the tightness of the coil. The limit on the rate of oxygen addition and carbon dioxide removal might be imposed, for thick-walled tubes, by the diffusion through the tube wall. The wall-limited case is governed by CO_2 removal.

List of symbols

C	concentration of oxygen or carbon dioxide in plasma
C_0	initial plasma oxygen or carbon dioxide concentration
C_∞	plasma oxygen or carbon dioxide concentration at the wall
D	diffusivity of oxygen or carbon dioxide
$f(C)$	sink term in oxygen balance, a function proportional to the slope of the oxyhemoglobin dissociation curve
F	function
K	helix radius
K^*	coil ratio
L	total length of tubing
L_i	length of tubes in the i^{th} stage
M	number of stages in an oxygenator
N_i	number of tubes in the i^{th} stage
N_{Re}	Reynolds number
N_{Sc}	Schmidt number
pCO_2	partial pressure of carbon dioxide
pO_2	partial pressure of oxygen
Q	blood flow rate
r	radial distance coordinate
r^*	dimensionless radial distance coordinate
R	radius of tube
R_i	inner radius of annulus
R_0	outer radius of annulus
S	local oxygen saturation of blood
$\bar{S}$	cup-mixed oxygen saturation of blood
S_0	initial saturation of blood
V	velocity of blood
V_m	cross sectional average velocity of blood
V_z	axial component of blood velocity
z	axial distance coordinate
z^*	dimensionless axial distance coordinate
ΔS_i	saturation increase of the i^{th} stage
ν	kinematic viscosity
θ	angular measure in cylindrical coordinates

INTRODUCTION

GAS TRANSFER in membrane oxygenators involves both the diffusion of gases through a membrane and the dispersion of gases within the flowing blood. The efficiency of the overall process depends not only on the membrane diffusion and the liquid dispersion, but also on the interactions of the membrane process and the liquid process. Investigations of the general operation of flat, layered membrane oxygenators have been reported in the past (BENVENUTO and LEWIS, 1959; CLOWES, HOPKINS and NEVILLE, 1956; GALLETTI and BRECHER, 1962; LEWIS, BENVENUTO and DEMETRAKOPOULOS, 1958). The present work is a theoretical and experimental study of blood oxygenation in units whose membranes are round tubes with gas-transmitting walls. The analysis of the performance of such a

† *Received* 15 *May*, 1968; *in revised form* 4 *November* 1968.
‡ Present address: Carnegie-Mellon University, Pittsburgh, Pennsylvania.

membrane oxygenator includes consideration of the transmission of gases through a membrane and the subsequent diffusion and convection of gases in the flowing blood.

In a generalized problem for oxygenator studies, the arbitrarily shaped membrane is in contact with an oxygen rich atmosphere on its outer surface and with flowing blood on its inner surface. The overall mass transfer rate depends on the gas partial pressures, the physical nature of the membrane and the diffusion and mixing of the oxygen within the flowing blood. The rate at which oxygen transfers through the membrane, for instance, depends on the difference between the partial pressure of the gas outside the membrane to that inside, the thickness of the membrane, and the physical properties of the membrane. At the entrance of an oxygenator the gas partial pressure gradient is determined by the entering blood saturation, the oxygen atmosphere present outside the membrane, and the chosen membrane material and thickness. Further downstream, however, the gas transfer through the tube wall, in addition to the above factors, depends on the oxygen buildup at the inside wall. To maintain a large gas partial pressure gradient across the wall and to keep the gas flowing through the membrane, the oxygen previously diffused through the membrane should be swept away from the inner surface by diffusive and/or convective mixing in the blood. As soon as the oxygen diffuses to the inside wall, it should be mixed with the centreline blood.

The present study emphasizes a general analysis of the transfer process. The results of such an analysis indicate limiting features of the innumerable alternative combinations of membrane geometry and flow kinematics. The results are applicable to many specific cases.

The general analysis is based on a mathematical statement of the physical principle that the mass of oxygen must be conserved. This statement asserts that for a steady condition there is no net gain or loss of oxygen anywhere in the flow. In passing through the tube some of the oxygen may combine with hemoglobin to form oxyhemoglobin, but the total mass of oxygen entering the tube, in all forms, must be equal to that leaving. The solution of the boundary value problem, specified by the differential equation and physically imposed boundary conditions, yields the oxygen content everywhere in the blood. In vector notation, the mass balance equation is

$$D\nabla^2 C = [1 + f(C)]\,[\boldsymbol{V} \cdot \nabla C], \qquad (1)$$

in which D is the diffusivity of oxygen in the blood or in the wall, depending on the region of problem being solved, C is the oxygen concentration, $\boldsymbol{V}$ is the oxygen velocity, and $f(C)$ is a function proportional to the slope of the oxyhemoglobin dissociation curve for the liquid phase problem and equal to zero for the membrane phase problem. The vector form is convenient since it is non-specific as to geometry or flow field.

The use of equation (1) to describe mass transfer in the liquid phase problem implies many basic assumptions. The red cells are assumed to behave like local reversible oxygen sinks, or depositories, that are convected in the flow. They are assumed to be uniformly distributed throughout the liquid. Equation (1) implies that the liquid is a homogeneous fluid and that the diffusion coefficient is independent of local gas pressure. The assumption that blood is a homogeneous fluid is not applicable to physiological gas transfer in which the diameters of the capillaries are of the same order of magnitude as the discrete dispersed red cells. In conduits having diameters at least two orders of magnitude greater than the dispersed phase elements, such as is true in most oxygenators, blood may be assumed to be a homogeneous fluid. As shown by other investigators (La Force, Conley and Fatt, 1962; Spaeth and Friedlander, 1967) under physiologic conditions an overall diffusion coefficient for blood is only slightly dependent on the local partial pressure and for high pressures the diffusion coefficient is essentially constant. In using equation (1) for the liquid phase problem, the left hand side represents the diffusing oxygen while the right

hand side represents the oxygen, dissolved as well as bound, carried in the flow. The sink properties of the red cells are non-linearly dependent upon the local plasma oxygen partial pressure and are taken into account in the mass balance by the term $f(C)$. The red cells are assumed to be in instantaneous equilibrium with the local plasma oxygen partial pressure and the instantaneous equilibrium is assumed to be given by the usual oxyhemoglobin dissociation curve. Other details of the derivation of equation (1) are given in an earlier paper (WEISSMAN and MOCKROS, 1967). The differences between the oxygenation and carbon dioxide removal problems involve the boundary and initial conditions, as well as the form of the sink term, $f(C)$.

At the blood-membrane interface there will be, in general, discontinuities in C, D, and derivatives of V. The presence of discontinuities adds to the complexity entailed in the solution of equation (1). A general understanding of the transfer process is most easily achieved by considering certain limiting cases of the problem. For instance, if the resistance to oxygen transfer offered by the membrane is appreciably less than that offered by the blood itself, the membrane may be neglected. In such cases, the oxygen tension at the outermost surface of the blood is assumed to be equal to that of the oxygen atmosphere. The transfer process is then limited by the fluid. If, on the other hand, the blood flow is such that all the gas coming through the wall is immediately carried away from the wall, either by rapid diffusion or fluid convection, the process is limited by the transfer rate through the wall. The first processes considered below, the flow limited cases, assume the wall can be made thin and permeable enough to be neglected in the analysis. Subsequently, the wall limited cases are considered.

Oxygenation in a straight round tube

The oxygenation of blood flowing laminarly in a straight round tube is considered most easily in cylindrical coordinates r, θ, and z. Assuming angular symmetry, a parabolic velocity profile in the tube, negligible axial diffusion, and negligible wall thickness, equation (1) reduces to:

$$D\left[\frac{\partial^2 C}{\partial r^2}+\frac{1}{r}\frac{\partial C}{\partial r}\right]=\left[1+f(C)\right]\left[2V_m(R^2-r^2)\right]\frac{\partial C}{\partial z} \tag{2}$$

in which R is the tube radius and V_m is the average blood velocity, the flow rate divided by cross-sectional area. Since sedimentation of the blood during passage through the tube is small, angular symmetry is reasonable. The assumption of zero tube wall thickness is justified if the tube wall resistance is much lower than that of the blood film. A parabolic velocity profile closely approximates the actual blood velocity profile at high shear rates and in large tubes. Even in small (40μ) tubes and at lower shear rates, a parabolic velocity profile is a reasonable first approximation to the actual profile. (BENNETT, GATSTEIN and SCHNECK, 1965; BUGLIARELLO and HAYDEN, 1963; MERRILL and PALLETIER, 1967). For tubes whose diameters are the size of physiological capillaries the parabolic velocity profile is clearly not valid. The smallest tube diameter used in the accompanying experiments was 0·025 in., or 635 μ, hence one would expect equation (2) to apply. If the plasma oxygen concentration is low, the oxygen velocity, for practical purposes, is equal to the blood velocity.

Associated with equation (2) are the conditions that the plasma oxygen concentration has some initial value, C_0, at the tube entrance and a final value, C_∞, at the wall. This final value is simply the wall pO_2 multiplied by the oxygen solubility in blood.

Despite the simplifying assumptions of the model, an analytical solution of equation (2) is not feasible at this time, and a numerical method of solution had to be adopted. The numerical solution is simplified by introducing the the dimensionless variables $r^* = r/R$ and $z^* = \pi Dz/2Q$, in which Q is the blood flow rate. These dimensionless variables permit the use of a single computer solution for all tube radii and flow rates. If dimensionless variables were not introduced, every tube size and flow rate of

interest would have a separate solution. More extensive details of the solution technique were given earlier (WEISSMAN and MOCKROS, 1967).

The oxygen saturation increase of a blood sample collected at the oxygenator exit is obviously important in design. The solution of the mass balance equation yields values of plasma oxygen concentration for points over cross-sections all along the tube length. Concentration values are converted to saturations using the oxyhemoglobin dissociation curve. Once obtained, the radially varying saturations must be averaged over the cross-section in a suitable fashion. The average saturation is computed on the basis of the volume of blood discharged through each area of the tube cross section. Thus, the average saturation of the exiting blood is:

$$\bar{S}(z^*) = \frac{\int_0^1 r^* S(r^*, z^*) V_z(r^*) dr^*}{\int_0^1 r^* V_z(r^*)\, dr^*}, \qquad (3)$$

in which $\bar{S}(z^*)$ is the average saturation, a function of the dimensionless tube length z^*; $S(r^*, z^*)$ is the unaveraged saturation, which varies with r^* and z^*; and $V_z(r^*)$ is the axial velocity. The bottom integral represents the total blood volume discharge from the tube exit. Equation (3) yields the saturation measured in a well-mixed sample collected at the tube exit. Since the variable r/R is removed by the integration and the variable $\pi Dz/2Q$ does not contain the tube radius, R, the average saturation is independent of the tube radius. In the integral of the numerator, the factor $r^* V_z$ weights the saturation contribution to the exiting sample from the various radii. Thus, high concentrations of oxygen at the wall and at $r^* = 0$ contribute little to the saturation of the collected sample.

Figure 1 shows computed oxygen concentration profiles for various situations. In all cases the blood enters the tube at $z^* = 0$ with an O_2 saturation of 75 per cent. Curve A is the profile for the laminar flow with the oxygen sinks, the model considered in this analysis. The location of the downstream profile was chosen such that the average saturation of an exiting sample is 90 per cent. If the velocity profile was assumed uniform, instead of parabolic, the saturation profile at the same distance downstream is given by curve B. For this case, however, the collected sample would have a saturation of 96 per cent. The considerably higher saturation is not due to the slight change of the profile, but, for the most part, to the much larger contribution to the sample made by the blood travelling near the wall. A parabolic velocity profile weights blood in the centre of the tube more heavily than does a profile with a uniform velocity. Since the tube axis is the last place reached by the diffusion front it would be expected, for tubes of equal size and flow rate, that a flat velocity profile would yield a more highly oxygenated blood sample than would a sample from a parabolic velocity profile. The weighting factor with the uniform velocity profile favors the highly concentrated blood at the wall. The uniform velocity profile that gives a 90 per cent saturated sample, occurring at a z^* much less than that for the parabolic profile, is shown as curve C.

The presence of the red cells materially affects the nature of the diffusion process. The red cell sinks tend to maintain a steep oxygen concentration front that moves inward toward the centre of the tube. The ordinary sinkless diffusion would give a concentration profile steep at the wall, but tending to flatten out as it moves inward. For comparison, the hypothetical profile that would occur if the sink effect were absent is shown by curve D on Fig. 1.

If the transfer of oxygen within the blood is very rapid compared to the transfer through the tube wall, the concentration within the blood will tend to even out. If the oxygen transfer rate in blood is infinitely fast, profile E would occur.

Meaningful solutions of the mass balance equation may be presented in the form of curves illustrating the variation of the average saturation of a well-mixed sample leaving a tube as functions of the dimensionless length z^*. Various physical factors affect the form of these curves. Among these are the velocity profile, total

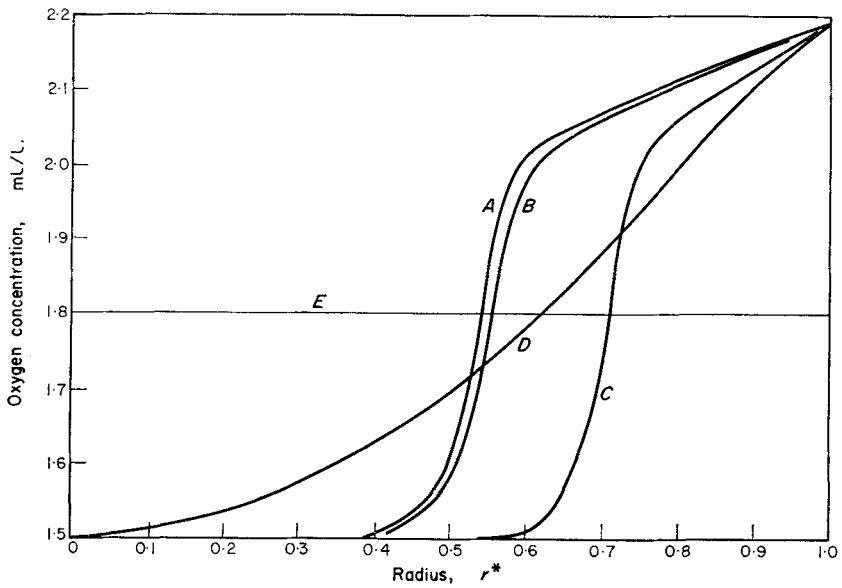

FIG. 1. Radial variation of oxygen saturation in straight tube. A = 90 per cent average saturation parabolic velocity profile, $z^* = 0{\cdot}122$; B = 96 per cent average saturation, uniform velocity profile, $z^* = 0{\cdot}122$; C = 90 per cent average saturation, uniform velocity profile, $z^* = 0{\cdot}059$; D = 90 per cent average saturation, parabolic velocity profile, without red cell oxygen sink effect, $z^* = 0{\cdot}053$; E = 90 per cent average saturation, infinite mixing.

hemoglobin content, initial oxygen saturation, and form of the oxyhemoglobin dissociation curve.

The hemoglobin content of the blood is reflected in the strength of the red cell oxygen sinks. Blood with a high hemoglobin content requires a longer tube to saturate than blood with low hemoglobin content, other things being equal. At any fixed saturation level the high hemoglobin blood, of course, contains more oxygen than the low.

The effect of the initial saturation on the solution is a consequence of the non-linearity of equation (2). If this equation were linear, a dimensionless concentration could have been introduced, allowing one solution to be valid for all initial saturations. Unfortunately, the presence of the term $f(C)$ makes the equation non-linear and eliminates this possibility, thus making a separate solution necessary for each initial saturation of interest. The shape of the oxyhemoglobin dissociation curve makes it easier to add oxygen to blood with low saturation than to blood with high saturation.

For fixed initial saturations and the high atmospheric oxygen tension the shape of the oxyhemoglobin dissociation curve has only a slight effect on the solution curves. Thus, the saturation vs. length curves obtained by using an $f(C)$ for one mammalian species at a specific pH and pCO_2 will be applicable, for practical purposes, to other species at other values of pH and pCO_2.

A more complete report of the effects of varying the above physical parameters on the solution curves was presented earlier (WEISSMAN and MOCKROS, 1967).

A series of experiments, using EDTA anticoagulated cattle blood flowing through silicone rubber tubes, was performed for the purpose of verifying the computer results. A 94 per cent oxygen, 6 per cent carbon dioxide gas was used

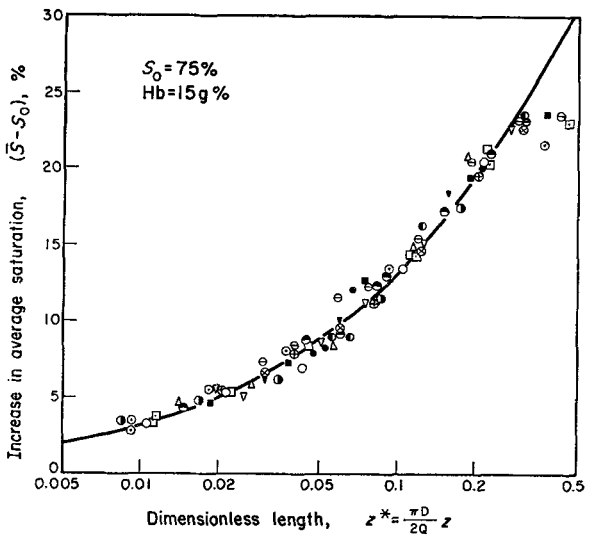

FIG. 2. Oxygen saturation increase as a function of the dimensionless axial length for straight silicone rubber tubes. The theoretical curve is the numerical solution of equation (2). Experimental points were located using an average diffusivity of $0{\cdot}89 \times 10^{-5}$ cm^2/sec and measured flow rates. △, ▼, ▽ ⊡, ⊙ are for tubes with lengths of 6′, 6′, 4′, 2′, and 2′, respectively, and with 0·08 in. I.D. × 0·09 in. O.D.; ◐, ● are for two experiments using 6′ of tube with 0·025 in. I.D. × 0·047 in O.D.; ■, ⊖, ◓, □ are for tubes with lengths of 6′, 6′, 4′, and 2′, and with 0·058 in. I.D. × 0·077 in. O.D.; ⊗, ⊕, ◑ are for tubes with lengths of 6′, 4′, and 2′, and with 0·04 in. I.D. × 0·085 in. O.D.; ○ is for a 2′ long tube with 0·25 in. I.D. × 0·375 in. O.D.

under one atmosphere of pressure. Data from these experiments along with the computer-obtained-theoretical solution for cattle blood, hemoglobin 15 g per cent, initial saturation 75 per cent, is shown in Fig. 2. For use in the theoretical computations, several experimental determinations were made of the bovine oxyhemoglobin dissociation curve. These experimental points were fit with two exponentials and the function $f(C)$ was taken from the fitted curve.

The oxygenation experiments utilized flow rates that ranged from 0·125cm^3/min to 38·2 cm^3/min. An oxygen diffusivity in blood of $5{\cdot}3 \times 10^{-4}$ cm^2/min, or $0{\cdot}89 \times 10^{-5}$ cm^2/sec, was used. This diffusivity was obtained by fitting experimental data to the dimensionless theoretical curve. It represents an average of the diffusivities observed in runs with eighteen different tubes. Each run consisted of pumping blood through a tube at five or six flow rates with two or three oxygen saturation measurements taken at each flow rate. The standard deviation observed was $\pm 0{\cdot}4 \times 10^{-4}$ cm^2/min (or $\pm 0{\cdot}07 \times 10^{-5}$ cm^2/sec). No correlation was seen between the observed diffusivities and any physical dimension or ratio of dimensions of the tubes tested. Thus, experiments using a 0·250 in. I.D. tube with a wall thickness to inner diameter ratio of 0·250, a 0·04 in. I.D. tube with a wall to diameter ratio of 0·563, and a 0·08 in. I.D. tube with a wall to diameter ratio of 0·0625 yielded nearly the same values of diffusivity. This constancy of diffusivity justifies neglecting the tube

wall in the analysis. The numerical value of the diffusivity obtained is close to other values reported in the literature (MARX, SNYDER, ST. JOHN and MOELLER, 1960; SPAETH and FRIEDLANDER, 1967).

In Fig. 2, saturations in excess of 100 per cent imply that all the hemoglobin present is fully oxygenated and excess oxygen is present in dissolved form. The experimentally measured oxygen saturations, being based on photometric principles, could not go above 100 per cent. Hence, the experimental points systematically deviate from the theoretical curve at saturations above 98 per cent.

Improving oxygen transfer in the liquid phase

For the laminar flow in a straight tube, discussed above, the oxygen transfer through silicone rubber tube walls of reasonable thickness is much faster than needed for the rate at which oxygen can diffuse into the flowing blood. The process is obviously improved by aiding the mixing or transfer of the oxygen in the liquid phase. An improved gas transfer in the blood, resulting in a more efficient process, would decrease the necessary length of tubing. A reduced tubing requirement, in turn, decreases the oxygenator priming volume. In the case of a straight tube, the oxygen diffusion front moves radially inward with decreasing velocity and slowly approaches the tube axis. With the front near the wall, the oxygen transfer is most rapid. Mixing of the blood tends to keep the diffusion front near the wall. In the presence of 'perfect' mixing, where oxygen concentration in the tube is not a function of the radial coordinate, blood takes up and uniformly mixes oxygen as fast as it comes through the wall. In such an instance, the oxygenator efficiency is limited only by diffusion through the tube wall.

Staging. If blood were allowed to flow laminarly through a straight tube, mixed by passing it through a manifold, and then allowed to flow laminarly through a second straight tube, the total increase in saturation at the exit of the second tube would exceed that obtainable with a single tube of equivalent length. Mixing, which occurs in the manifold, returns blood with uniform oxygen concentration to the second tube and starts the diffusion front moving inward from the tube wall once again. This staging process effectively increases the oxygenation rate by increasing the average velocity of the diffusion front.

As the number of stages used approaches infinity it follows that the length of each stage approaches zero. Thus, the condition of 'perfect' mixing is approached throughout the tube by the use of many stages. In theory the amount of tubing and hence the priming volume required could be reduced to zero by use of an infinite number of stages, In practice, however, stages are limited to a finite number. A considerable saving of tubing, however, could be effected by staging.

For a fixed number of stages and saturation increment, the length of each stage for optimum oxygen transfer is of interest. For diffusion in the absence of a chemical reaction, the stages should be of equal length. The non-linearity imposed by the oxygen reaction invalidates this result, and the determination of optimum stage lengths for more than two stages is a tedious process.

If the oxygenator is to have M stages and is to raise the saturation by ΔS for a flow rate Q, it is of interest to determine how many tubes, N_i, and what length, L_i, should make the i^{th} stage, so that the total length of tubing used, L, is minimized. The saturation increase for the i^{th} stage is a function, F, of z_i^*, the dimensionless length for the i^{th} stage. For each tube z_i^* is $\frac{\pi D}{2(Q/N_i)} L_i$, thus:

$$\Delta S_i = F\left(\frac{\pi D}{2Q} N_i L_i\right), \tag{4}$$

where N_i, L_i, and ΔS_i are the number and length of the tubes and the saturation increase, respectively, for the i^{th} stage, and F is an unknown function. In other words,

$$N_i L_i = \frac{2Q}{\pi D} F^{-1}(\Delta S_i). \tag{5}$$

Thus, for some unknown but constant value of ΔS_i corresponding to optimization, the total length of tubing per stage is fixed, but the number of tubes is arbitrary. For the complete oxygenator:

$$L = \sum_{i=1}^{M} N_i L_i = \frac{2Q}{\pi D} \sum_{i=1}^{M} F^{-1}(\Delta S_i), \qquad (6)$$

and for minimum L:

$$\frac{\partial L}{\partial S_i} = 0 \quad i = 1, M-1, \qquad (7)$$

in which S_i is the average saturation at the exit of the i^{th} stage.

An approximate solution of equation (7) for two stages between 75 and 95 per cent oxygen saturation shows that a 33 per cent saving of tube length is effected. This saving could, of course, increase markedly with the number of stages used, but at the expense of more complex fabrication.

Turbulent mixing. Turbulence is another means of creating mixing within the tube. A solution for the concentrations in a straight tube in the presence of fully established turbulent flow is given by JAKOB (1949, see LATZKO therein) for the case of infinitely thin-walled tubes. This solution for the linear case (no sinks), is based on the $1/7^{th}$ power law velocity distribution and the Von Karman-Prandtl turbulent diffusivity. It is easily averaged over the tube cross section and velocity to find the properties of a well-mixed sample leaving the tube exit. An upper bound on the length of tubing needed to oxygenate blood in the presence of turbulence can be obtained using the Latzko solution with the axial length z replaced by z times $[1 + f(C_0)]$. A comparison of this upper bound with the oxygen transfer through the tube wall for a 0·085 in. O.D. × 0·040 in. I.D. silicone rubber tube with a flow rate of 610 cm³/min, a blood viscosity of 0·042 cm²/sec, an initial saturation of 75 per cent, and a final saturation of 105 per cent, indicates that turbulence is very effective in reducing the problem to one in which oxygenation is limited by diffusion through the tube wall. If the gas transfer through the wall is unimportant, the length of tubing needed in the turbulent case is only 0·06 per cent of that needed in the laminar flow. The flow rate necessary to create the turbulent flow would create excessive head losses and shearing stresses, however.

In spite of the improved oxygen transfer gained through the introduction of turbulence, its use would be contraindicated by studies (BLUESTEIN and MOCKROS, to be published; YARBOROUGH, MOCKROS and LEWIS, 1966) showing that considerable damage to the formed elements of the blood can result in high Reynolds number flows.

Helical coiling. Coiling the tube axis in the form of a helix results in a third method of introducing mixing. Because of centrifugal forces, the coiling generates a secondary velocity in the cross sectional plane of the tube. The secondary velocities for the laminar flow of a Newtonian fluid in a coiled tube were determined by DEAN (1927). For the high shear rates involved in an artificial lung, blood is essentially a Newtonian fluid. These secondary velocities (see Fig. 3) convect oxygen laden blood from the tube surface to the tube interior. Near the tube centre the oxygen is released to the surroundings more rapidly than it could diffuse in from the wall. Also, away from the wall the axial velocity

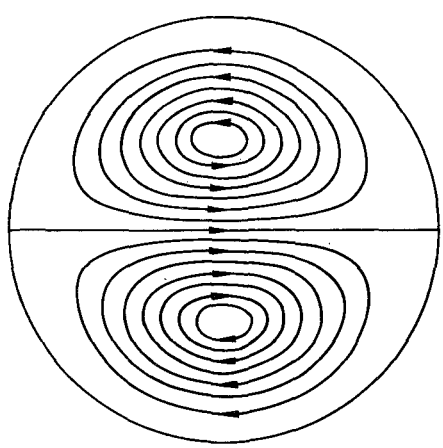

FIG. 3. Secondary velocities in the cross section of a coiled tube.

is larger, making that portion important in the exit sample. Additionally, the presence of convection moves low saturation blood from the interior to the wall, where it is readily oxygenated. This mass transfer problem is described in equation (1) with the appropriate velocities inserted.

The boundary conditions for this problem are that the concentration is uniform and equal to C_0 for z less than zero; that the concentration at the wall is C_∞; and that symmetry exists about the plane $\theta = \pm \pi/2$.

An advantageous equation descriptive of this problem is achieved by introducing the dimensionless parameters, Reynolds number, N_{Re}, Schmidt number, N_{Sc}, and the coil ratio, K^*, and the dimensionless variables r^* and z^*:

$$N_{Re} = \frac{2Q}{\pi R \nu}; \qquad N_{Sc} = \frac{\nu}{D}; \qquad K^* = K/R;$$

$$r^* = \frac{r}{R}; \qquad z^* = \frac{z}{R},$$

in which ν represents the blood viscosity and K the helix radius. Thus, in nondimensional cylindrical coordinate's equation (1) becomes

$$\frac{\partial^2 C}{\partial r^{*2}} + \frac{1}{r^*}\frac{\partial C}{\partial r^*} + \frac{1}{r^{*2}}\frac{\partial^2 C}{\partial \theta^2} + \frac{\partial^2 C}{\partial z^{*2}} =$$

$$[1 + f(C)]\left\{\frac{N_{Re}^2 N_{Sc} \sin\theta}{288K^*}(1 - r^{*2})^2 (4 - r^{*2})\frac{\partial C}{\partial r^*}\right.$$

$$+ \frac{N_{Re}^2 N_{Sc} \cos\theta}{288K^*}(1 - r^{*2})(4 - 23r^{*2}$$

$$+ 7r^{*4})\frac{1}{r^*}\frac{\partial C}{\partial \theta} + N_{Re} N_{Sc}(1 - r^{*2}) \times \qquad (8)$$

$$\left.\left[1 - \frac{3r^* \sin\theta}{4K^*} + \frac{N_{Re}^2 \sin\theta}{11520K^*} \times (19r^* - 21r^{*3}\right.\right.$$

$$\left.\left. + 9r^{*5} - r^{*7})\right]\frac{\partial C}{\partial z^*}\right\}.$$

An alternative form of this equation may be obtained by defining z^* as in the straight tube flow solution. This alternate form is not as physically appropriate as the form adopted. In the straight tube case, however, it led to an elimination of parametric dependence (Weissman and Mockros, 1967).

The solution of the problem was simplified by considering that the effects of coiling could be accounted for by using the secondary velocities in a straight tube and by using the symmetry about the plane $\theta = \pm \pi/2$. The governing differential equation has three dimensionless parameters, is three dimensional and non-linear, and has spatially variable coefficients. The addition of r and θ velocities greatly increases the computer time required to effect a solution over that needed for the straight tube problem. Equation (8) was solved using an implicit finite difference numerical solution technique. The special and involved details of the solution scheme are given in another paper (Weissman and Mockros, 1968)†. The solution of this equation gives concentrations and saturations at each of the finite-difference-grid points in the half circular region $|\theta| \leq \pi/2$, $r^* \leq 1$, for each value of z^* down the tube.

Figure 4 shows the $r - \theta$ saturation contours for an average saturation of 90 per cent in the case with a Reynolds number of 20, a Schmidt number of 4750, and a coil ratio of 10. The saturation contours were constructed by interpolating between the saturation values computed

† The finite-difference-grid used for the solution reported in Weissman and Mockros, 1968, consisted of 118 points (9 on each of 13 radii and one centre point) in the half circular region. Although that solution was extensively tested for discretization errors in the z direction, limits of computer time precluded an extensive study of discretization errors in the $r - \theta$ plane. In subsequent work, the efficiency of the computer program was improved in such a way as to permit considerable refinement of the grid. The refined programs used finite-difference-grids of as many as 1912 points (39 points on each of 49 radii and one centre point). Although the results from the two solutions are different, the solution using 1912 points verifies the general correctness of the solution using 118 points. The contours plotted on Fig. 4 are those from the 1912 point solution. For comparison, the curves that resulted from the use of various grids are plotted on Fig. 5. The curve plotted on Fig. 6 is based on the 118 point solution.

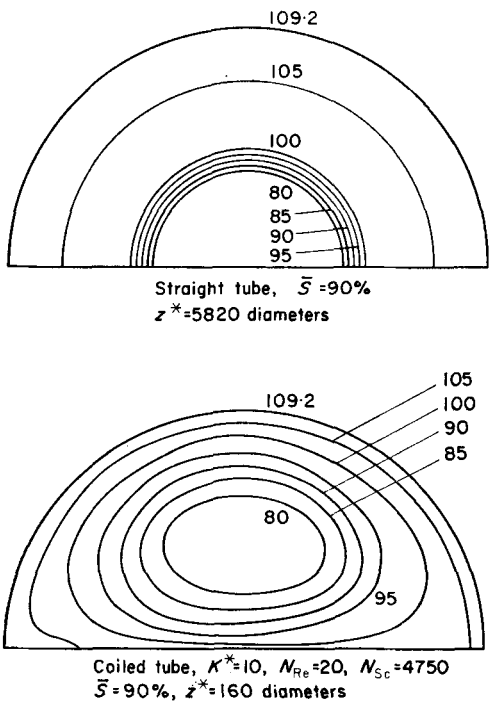

FIG. 4. Saturation contours for the straight tube and a coiled tube. The contours for the coiled tube are based on the 1912 grid-point solution. (See footnote on p. 177.)

at the grid points. Also shown are the comparable concentration contours for the straight tube flow without cross sectional convection. The degree of spread in the contour lines brought about by the circulatory mixing indicates the effectiveness of the coiling. The cross section shown for the straight tube flow is much further downstream than the cross section shown for the coiled tube.

Using a method similar to that described for the straight tube, the average saturation of an exiting sample can be computed for each z^*. The saturation values at each of the grid points are weighted according to their volume contribution to an exiting sample. The weighted saturations are integrated over the area and divided by total blood volume discharge to yield an average saturation for the exiting sample.

The solution of the coiled tube problem, for typical values of the dimensionless parameters, indicates that coiling is very effective in mixing the blood and producing a much more saturated exiting sample. The results indicate, for example, that with a Reynolds number of 20, a Schmidt number of 4750, and a coil ratio of 4, the coiled tube needs to be only 1·3 per cent of the length of the straight tube if $S_0 = 75$ per cent and $\Delta S = 20$ per cent.

Figure 5 indicates that decreasing K^*, i.e. making the coil tighter, at a constant N_{Re} of 20 leads to an increase in the oxygenation rate. The straight tube solution, $K^* = \infty$, is included in Fig. 5 for comparison. The dimensionless length used for the straight tube solution may be converted to diameters by multiplying by $\frac{1}{2}N_{Re}\,N_{Sc}$. The effect of decreasing K^* is to increase the convective $r - \theta$ velocities, and hence the observed variation of the solution with K^* might be expected.

Varying the Reynolds number results in two conflicting effects. Increasing the Reynolds number causes a linear increase in both the $r - \theta$ convective velocities and the axial velocity. The increased axial velocity leads, for a fixed length of tube, to a decrease in the radial penetration of the diffusion front. The decrease in diffusion penetration implies that fewer of the convected oxygen sinks will be carrying oxygen to the tube interior. On the other hand, because of increased $r - \theta$ velocities, the sinks which do carry oxygen will be more effective. The conflicting effects of Reynolds number variation suggest that the solution will be less sensitive to Reynolds number changes than to changes of K^*. This behavior is explored in a previous paper (WEISSMAN and MOCKROS, 1968) for a coil ratio of 10. It might be expected that some optimum Reynolds number for oxygen transfer exists. At low values of Reynolds number the solution reduces to that of the inefficient straight tube. At high Reynolds numbers, diffusion effects cannot penetrate far into the cross section of a tube of fixed length. With $r - \theta$ convection velocities small near the wall, convection will not be effective in increasing the oxygenator efficiency at these high Reynolds numbers. Between these two extremes convection speeds oxygenation. The previous study (WEISSMAN and MOCKROS, 1968)

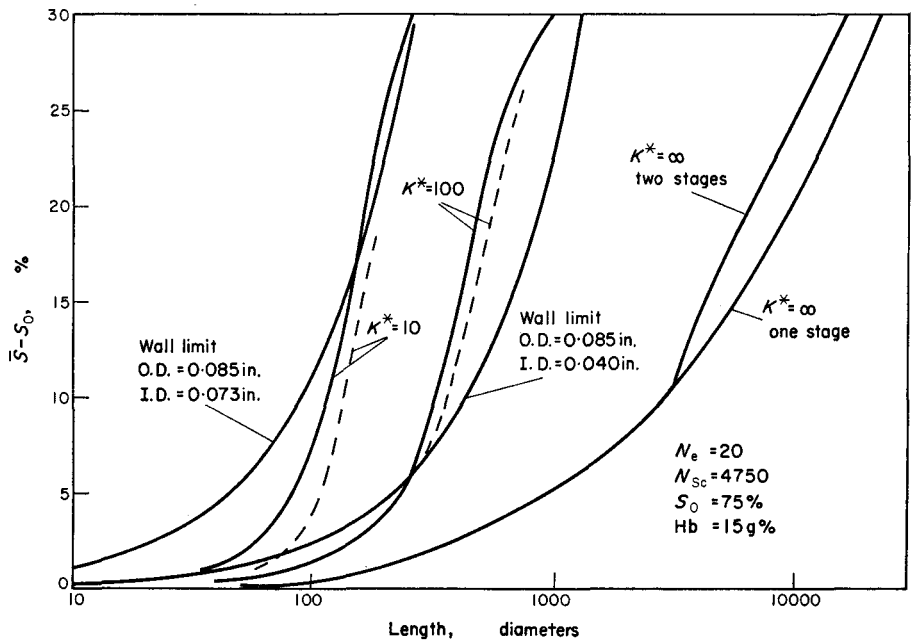

FIG. 5. Oxygen saturation increase as a function of length in diameters for several limiting cases. All curves are for a Reynolds number of 20 and a Schmidt number of 4750. For coiled tubes: ———— results based on 118 grid-point solution; — — — — — — results based on finer grids, 508 points for $K^* = 100$ and 1912 points for $K^* = 10$. (See footnote on p.177.)

indicates that with a Schmidt number of 4750 and a coil ratio of 10 the optimum Reynolds number lies between 10 and 40, since the solution for a Reynolds number of 20 is more efficient than those for either 10 or 40. Without more information it is not possible to tell whether this optimum is relative or absolute.

As might be expected, an increase of the Schmidt number, corresponding physically to either increased blood viscosity or decreased diffusivity, leads to a less efficient oxygenation process. The previous paper (WEISSMAN and MOCKROS, 1968) shows this behavior for flows with a Reynolds number of 20, a coil ratio of 10, and with Schmidt numbers of 4750 and 7500.

Carbon dioxide elimination

Carbon dioxide elimination is treated similarly to oxygenation. Although again involving the appropriate form of equation (1), the mathematics of the flow limited process is simplified in the case of carbon dioxide removal because of the form of the sink term $f(C)$. The narrow range of partial pressures allows the approximating of the essential part of the CO_2 absorption curve by a straight line. Such an approximation makes the problem linear and the solution much simpler. Advantage of the linearity of the CO_2 removal equation is taken by replacing the concentration C in equation (8) with a dimensionless concentration $C^* = (C - C_0)/(C_\infty - C_0)$. The earlier study (WEISSMAN and MOCKROS, 1967) showed that for the straight flow the length of tubing needed to eliminate CO_2 is less than the length needed to raise the saturation from 75 per cent to 98 per cent for blood with a 15 g per cent total hemoglobin. Thus, the straight tube oxygenator is not CO_2 limited.

In the coiled tube case, the boundary conditions for the flow limited process are that C^* equals one for z less than zero, that C^* equals zero at the wall, and that the solution is symmetrical about a diametral plane. Solutions for

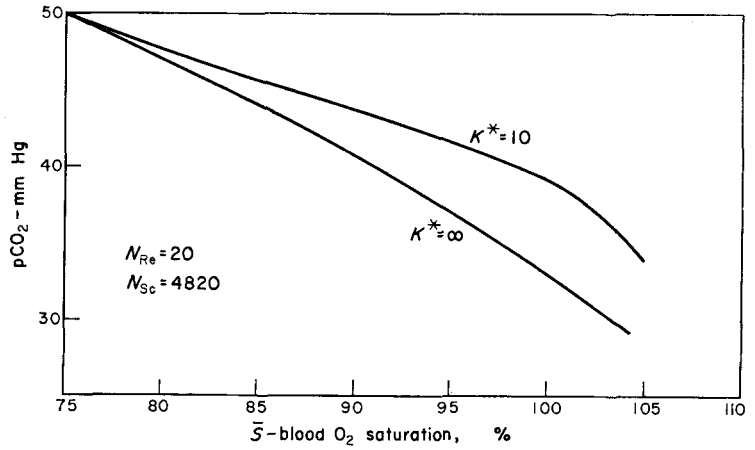

FIG. 6. Carbon dioxide removal compared with oxygenation for the straight tube and a tube coiled with $K^* = 10$. Curve for coiled tube is based on 118 grid-point solution. (See footnote on p. 177.)

CO_2 removal in the coiled tube were obtained corresponding to the oxygenation solutions mentioned above. Examination of the CO_2 removal reveals that for the coiled tube, lowering pCO_2 from 50 to 40 mm Hg, requires the oxygen saturation to rise higher than 96 per cent. This indicates that the oxygenation process for the coiled tube is limited slightly by CO_2 removal. As discussed below, however, the coiled tube oxygenator may become wall limited, in which case it becomes even more strongly CO_2 limited. Figure 6 shows pCO_2 plotted against oxygen saturation for the flow through a straight tube and for a flow with a Reynolds number of 20 through a tube with a coil ratio of 10. Both solutions assume an infinitely-thin-walled tube.

The wall effect

For the tube sizes used in the straight tube experiments the full advantage offered by the turbulent mixing or the coiling is masked by the limit imposed on oxygen transfer by the tube wall diffusion. For example, the above solution with a coil ratio of 4 and a Reynolds number of 20 indicates that only 6 in. of 0·085 in. × 0·040 in. silastic tubing is needed to raise blood from 75 per cent to 100 per cent saturation. The coiling, however, generates such an efficient internal mixing that the assumption (used in the solution) that the wall has no effect is no longer valid. In fact, with perfect internal mixing, i.e. all oxygen coming through the wall instantaneously mixing throughout the flow cross section, the tube wall admits only enough oxygen to raise the saturation to 78 per cent in this 6 in. length. Furthermore, the less than perfect mixing in the tube with $K^* = 4$ allows even less oxygen to pass through the wall.

Perfect mixing is another of the limiting problems studied; perfect mixing is the wall limited process. It represents the upper limit placed on the practical case by the wall diffusion. The wall limited case is governed by the steady state diffusion through an annulus, the cross section of wall. The increase in total blood oxygen concentration in this case is given, approximately, by:

$$O_2 \text{ increase} = \frac{2\pi D\, \Delta C L}{\ln\left[\frac{R_o}{R_i}\right]} \frac{\text{moles}}{\text{min}},$$

in which ΔC is the average concentration gradient across the tube wall and equals the pO_2 gradient times the oxygen solubility in the wall material, R_0 and R_i are inside and outside radii of the tube, respectively, L is the tube length, and D is the diffusivity of oxygen in the tube wall. The product of the oxygen diffusivity with solubility

for silicone rubber is $1 \cdot 195 \times 10^{-8}$ moles/cm min atm (Dow Corning Corporation, 1959).

Coiled tube oxygenation experiments

Experiments were performed, using apparatus similar to that for the straight tube to determine if coiling of the oxygenating tubes was effective in increasing oxygenator efficiency. These experiments were performed using three tube sizes, 0·058 in. × 0·077 in., 0·0918 in. × 0·0718 in., and 0·085 in. × 0·075 in. The lengths tested ranged from 18 in. to 12 ft and the coil ratio used was 12. Experiments were conducted at flow rates of 1·91 to 38·2 cm³/min. The oxygen atmosphere was the same as previously used.

In all of the experiments, the coiling significantly improved oxygenator efficiency. For any particular saturation increase, the ratio of the straight tube length to the length needed in the improved process is called the improvement factor. An upper bound on the improvement factor is determined by either the theoretical coiled tube solution for the fluid with zero wall thickness or the solution for oxygen transfer across the tube wall with perfect fluid mixing, whichever is lower. The observed improvement factor is the ratio of the theoretical straight tube length to the actual length used. For several reasons the observed saturation increase must be less than either of the ideal limits. The most important of these in the wall limited case is that, although the coiling induces mixing, perfect mixing does not exist inside the tube and the oxygen gradient across the tube wall is therefore lower than assumed. The observed oxygenation is decreased further because the circulating velocity profile is not established immediately in the entrance section of the tube. Also, from a practical standpoint, not all of the surface was exposed to oxygen, since the tube was wound on a solid form. Furthermore, coiling tends to deform the cross sections of circular thin walled tubes into ellipses, and tubes with elliptical cross sections can exhibit decreased efficiency. In the experiment with the thinnest walled tube the observed improvement factor was found to be as high as 26·2. (The fact that this observed value is slightly greater than the theoretical upper bound is probably due to experimental error.)

For a fixed tube length, tube size, K^*, and N_{Sc} it was found that the observed efficiency increased with the flow rate. At higher flow rates the mixing in the tube was better and the wall limited case was more closely approached. For very high flow rates the efficiency will go down because of insufficient residence time for the blood in the tube. This effect was not observed at the flow rates investigated.

Table 1. Comparative oxygen transfer

$N_{Sc} = 4750$

O.D. (in.)	I.D. (in.)	Length (in.)	K^*	N_{Re}	ΔS (%)	Improvement factor Observed	Wall lim.	Flow lim.
0·077	0·058	144	12	6·55	20·7	1·4	30	18
				13·1	17·7	2·1	27	33
				52·5	11·1	3·6	19	65
				131·0	11·2	9·2	19	155
0·0918	0·0718	75	12	10·6	17·0	3·7	30	25
				20·8	11·5	3·6	22	30
				42·5	10·0	5·9	20	49
				106·0	9·5	13·6	20	114
0·085	0·073	18	12	10·4	10·0	6·1	33	13
				20·4	8·5	9·1	29	21
				41·7	7·0	13·6	26	33
				104·0	6·0	26·2	24	76

Table 1 presents a summary of fluid limited, tube limited, and observed improvement factors for the three tube sizes tested. The thinnest tube is the most efficient. The thickest tube is the least efficient in oxygenating the blood.

DISCUSSION

The practical efficiency of any oxygenator is limited by the materials available and the ingenuity of the designer. In a tubular membrane unit, the efficiency is limited by the gas conductivity and the physical strength of the membrane material, and the convective characteristics of the flow.

Silicone rubber is so transmissible to O_2 that for almost all tubes of reasonable wall thickness and internal diameter, the O_2 gets through so fast that straight flows are limited only by the gas dispersion in the fluid. Thus, a straight tube oxygenator could not be improved by using a thinner-walled tube. Improved design is achieved by inducing convective mixing in the flow. Although several techniques are available for inducing cross mixing, a simple and easily implemented method is to coil the tube. The analysis of the coiled tube flow shows that the coil does not have to be very tight before the mixing is sufficient to transport effectively the oxygen coming through the wall. With a slight amount of coiling, then, the process becomes limited by the O_2 transfer through the wall. Further improvement of the design is achieved by improving the wall transfer, e.g. use of thinner walled tubes. Tubes with very thin walls, however, have little structural rigidity and kink easily when coiled. Extruded tubes with a permanently set coil, being less prone to kinking, could be used to advantage. Staging also could be used in conjunction with a coiled tube oxygenator. The advantage of staging a coiled tube unit, however, would be less than that in a straight tube oxygenator. The oxygenation process is finally limited by how thin the tube wall can be made, retaining structural strength, and how tightly the coil can be wound.

Figure 5 shows the increase in blood O_2 saturation for several limiting cases, at a Reynolds number of 20. Saturation curves are shown for a straight tube, a two stage straight tube, a coiled tube with $K^* = 100$, and a coiled tube with $K^* = 10$, all for the hypothetical infinitely thin-walled tubes. Also shown are two saturation curves for the limit imposed by the wall when the fluid is always completely mixed. The latter curves are for the thinnest and thickest walled tubes tested. The wall-limited curves for even thinner walled tubes would be to the left and those for thicker walled tubes to the right of the curves shown.

The length of straight tubing needed to raise the saturation a designated amount is proportional to the Reynolds and Schmidt numbers. For blood at ordinary temperatures in a particular tube, the length is thus proportional to the flow rate. The length needed to raise the saturation a certain amount in a particular tube for the wall limited process also depends on the flow rate. Thus, for higher Reynolds numbers the straight tube curve and the wall limited curves are to the right of those shown in Fig. 5. For lower Reynolds numbers the curves are to the left. The curves translate a distance proportional to the flow rate change. For any particular tube (with a design coil tightness, membrane thickness, etc.) the experimentally observed oxygen saturation must lie to the right of either its wall limit curve or its flow limit curve, whichever is further to the right.

The above studies of flow-limited cases, indicate that the length of tube needed to eliminate CO_2 is about the same as the length needed to add sufficient oxygen. If, however, a particular model is limited by the wall transfer, the use of the unit as an artificial lung, both oxygenating and reducing CO_2, would be limited by the CO_2 removal. MELROSE *et al.*, (1958) pointed out that many common membrane materials are four times more permeable to CO_2 than to O_2 but that oxygen usually has a 15 to 1 partial pressure gradient advantage, i.e. $\Delta PO_2 = 750$ mm Hg and $\Delta CO_2 = 50$ mm Hg. The combination makes the wall transfer case limited by CO_2 transfer. Hyperbaric oxygen pressure could aid in transferring oxygen, but again the advantage

is lost in an oxygenator that is carbon dioxide limited.

The analysis and experiments indicate that a tubular membrane oxygenator is practical and, in some ways, advantageous.

Acknowledgment—This work was supported by funds awarded to Northwestern University by the National Institutes of Health under Grant Nos HE09536 and FR 00018, and GM 19418.

REFERENCES

BENNETT, L., GATSTEIN, H. and SCHNECK, D. (1965) Velocity profile determination for flowing blood, *Rev. Scient. Instrum.* **36,** 625.

BENVENUTO, R. and LEWIS, F. J. (1959) Influence of some physical factors upon oxygenation with a plastic membrane oxygenator. *Surgery* **46,** 1099.

BLUESTEIN, M. and MOCKROS, L. F. Hemolytic effects of energy dissipation in flowing blood. *Med. & Biol. Engng* **7,** 1–16.

BUGLIARELLO, G. and HAYDEN, J. W. (1963) Detailed characteristics of the flow of blood *in vitro*. *Trans. Soc. Rheol.* **7,** 209.

CLOWES, G. H., Jr., HOPKINS, A. L. and NEVILLE, W. E. (1956) An artificial lung dependent upon diffusion of oxygen and carbon dioxide through plastic membranes. *J. thorac. Surg.* **32,** 630.

DEAN, W. R. (1927) Note on the motions of fluid in a curved pipe. *Phil. Mag.* **4,** 208.

Dow Corning Corporation. *Gas Transmission Rates of Plastic Films*, July 1, 1959.

GALLETTI, P. M. and BRECHER, G. A. (1962) *Heart Lung Bypass*, Grune & Stratton.

JAKOB, M. (1949) *Heat Transfer*, Vol. I, Wiley.

LA FORCE, CONLEY, R. and FATT, I. (1962) Steady-state diffusion of oxygen through whole blood. *Trans. Faraday Soc.* **58,** 1451.

LEWIS, F. J., BENVENUTO, R. and DEMETRAKOPOULOS, N. (1958) A new pump-oxygenator employing polyethylene membranes. *Quart. Bull. Nwest. Univ. med. Sci.* **32,** 262.

MARX, T. I., SNYDER, W. E., ST. JOHN, A. D. and MOELLER, C. E. (1960) Diffusion of oxygen into a film of whole blood, *J. appl. Physiol.* **15,** 1123.

MELROSE, D. G., BRAMSON, M. L., OSBORN, J. J. and GERBODE, F. (1958) The membrane oxygenator, *The Lancet* **1,** 1050.

MERRILL, W. and PELLETIER, G. H. (1967) Viscosity of human blood: transition from Newtonian to non-Newtonian. *J. appl. Physiol.* **23,** 178.

SELLARS, J. R., TRIBUS, M. and KLEIN, J. S. (1956) Heat transfer to laminar flow in a round tube or flat conduit —the Graetz problem extended. *Trans. Am. Soc. mech. Engrs* **78,** 441.

SPAETH, E. E. and FRIEDLANDER, S. K. (1967) The diffusion of oxygen, carbon dioxide, and inert gas in flowing blood. *Biophys. J.* **7,** 827.

WEISSMAN, M. H. and MOCKROS, L. F. (1967) Oxygen transfer to blood flowing in round tubes. *J. Engng Mech. Div. Am. Soc. civ. Engrs* **93,** 225.

WEISSMAN, M. H. and MOCKROS, L. F. (1968) Gas transfer to blood flowing in coiled circular tubes. *J. Engng Mech. Div. Am. Soc. civ. Engrs* **94,** 957.

YARBOROUGH, K. A., MOCKROS, L. F. and LEWIS, F. J. (1966) Hydrodynamic hemolysis in extracorporeal machines. *J. thorac. and cardiovasc. Surg.* **52,** 550.

TRANSFERT DE L'OXYGENE ET DU GAZ CARBONIQUE DANS LES OXYGENATEURS A MEMBRANE

Sommaire—Le transfert des gaz dans les oxygénateurs à membrane peut être limité par la dispersion du liquide ou la diffusion de la membrane. S'il est limité par la dispersion du liquide, l'accroissement de la saturation moyenne d'oxygène du sang circulant dans des tubes rectilignes poreux dépend du débit, de la longueur du tube, du coefficient de diffusion, et est indépendant du diamètre du tube. Il est surprenant de noter que la solution mathématique se trouve être insensible aux dérives de la courbe de dissociation de l'oxyhémoglobine. Les hypothèses retenues pour le modèles et pour la solution analytique sont vérifiées par une série d'expériences utilisant du sang d'animaux. La succession de tubes, les turbulences et la courbure des tubes provoque un brassage qui augmente le taux d'oxygénation de façon significative. Pour les tubes en serpentin, l'efficacité de l'oxygénation dépend du nombre de Reynolds, du nombre de Schmidt et de l'étroitesse du serpentin. La limite au taux d'addition d'oxygène et à l'élimination de gaz carbonique peut être imposée au moyen de la diffusion à travers la paroi, pour les tubes à parois épaisses. C'est l'élimination du gaz carbonique qui régit cette limitation par la paroi.

SAUERSTOFF- UND KOHLENDIOXYDÜBERTRAGUNG IN MEMBRANOXYGENATOREN

Zusammenfassung—Die Gasübertragung in Membranoxygenatoren kann durch die Flüssigkeitsdispersion oder die Membrandiffusion limitiert werden. Liegt die Begrenzung in der Flüssigkeitsdispersion, so hängt der Anstieg der durchschnittlichen Sauerstoffsättigung des in geraden

gaspermeablen Schläuchen fließenden Blutes von der Strömungsgeschwindigkeit, der Schlauchlänge und dem Diffusionskoeffizienten ab, während er vom Schlauchdurchmesser unabhängig ist. Die mathematische Lösung ist erstaunlich unempfindlich gegenüber Verschiebungen in der Oxyhämoglobin-Dissoziationskurve. Die in dem Modell und in der analytischen Lösung benutzten Annahmen wurden in einer Reihe von Versuchen mit Rinderblut bestätigt. Durch entsprechende Lagerung und Wickelung der Schläuche und durch Turbulenz wird gemischt und eine bedeutende Verbesserung der Oxygenationsgeschwindigkeit erzielt. Bei gewickelten Schläuchen hängt die Wirksamkeit der Oxygenation von der Reynoldschen Zahl, der Schmiatschen Zahl und der Enge der Wicklung ab. Bei dickwandigen Schläuchen kann eine Geschwindigkeitsbegrenzung der Sauerstoffzugabe und der Kohlendioxydabgabe per Diffusion durch die Schlauchwand gegeben sein. Der wandbegrenzte Fall ist von der CO_2-Entfernung gesteuert.